Strong coupling between chlorosomes of photosynthetic bacteria and a confined optical cavity mode

Strong coupling between the chlorosome of a photosynthetic bacteria and a confined optical cavity mode

David M Coles,[†] Yanshen Yang,[‡] Yaya Wang,[‡] Richard T Grant,[¶] Robert A Taylor,[§] Semion K Saikin,[*,‖,⊥] Alán Aspuru-Guzik,[‖] David G Lidzey,[¶] Joseph Kuo-Hsiang Tang,[*,‡] and Jason M Smith[*,†]

Department of Materials, University of Oxford, Parks Road, Oxford OX1 3PH, UK, Department of Chemistry and Biochemistry, Clark University, Worcester, MA 01610-1477, USA, Department of Physics & Astronomy, University of Sheffield, Hicks Building, Hounsfield Road, Sheffield S3 7RH, UK, Department of Physics, University of Oxford, Parks Road, Oxford OX1 3PU, UK, and Department of Chemistry and Chemical Biology, Harvard University, 12 Oxford Street, Cambridge, MA 02138, USA

E-mail: saykin@fas.harvard.edu; JTang@clarku.edu; jason.smith@materials.ox.ac.uk

[*]To whom correspondence should be addressed

[†]Department of Materials, University of Oxford, Parks Road, Oxford OX1 3PH, UK

[‡]Department of Chemistry and Biochemistry, Clark University, Worcester, MA 01610-1477, USA

[¶]Department of Physics & Astronomy, University of Sheffield, Hicks Building, Hounsfield Road, Sheffield S3 7RH, UK

[§]Department of Physics, University of Oxford, Parks Road, Oxford OX1 3PU, UK

[‖]Department of Chemistry and Chemical Biology, Harvard University, 12 Oxford Street, Cambridge, MA 02138, USA

[⊥]Institute of Physics, Kazan Federal University, 18 Kremlevskaya Street, Kazan, 420008, Russian Federation

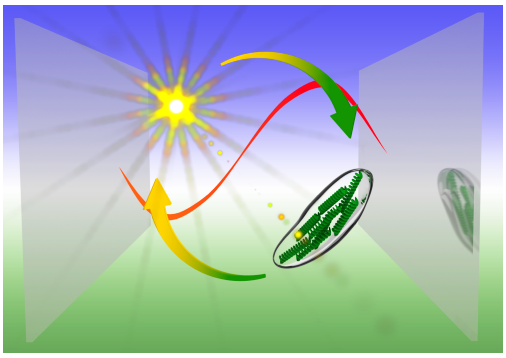

TOC image

Abstract

We demonstrate strong exciton-photon coupling between light-harvesting complexes and a confined optical mode within an optical microcavity. The energetic anticrossing between the exciton and photon dispersions characteristic of strong coupling is observed in reflectivity and transmission with a Rabi splitting energy on the order of 150 meV, which corresponds to about 1000 chlorosomes coherently coupled to the cavity mode. We believe that the strong coupling regime presents an opportunity to modify the energy transfer pathways within photosynthetic organisms without modication of the molecular structure.

Green sulfur bacteria grow anaerobically in sulfur-rich environments and are often found at the very lowest levels of the photic zone, such as in the bottom of stratified lakes, deep in the sea, and near geothermal vents.[1] In such ecological niches, each bacterium may receive only a few hundred photons per second.[2–4] Thus, it is generally assumed that the light-harvesting complex (LHC) of these bacteria has evolved to efficiently collect and use the small amount of light available.

The main optical antenna structures in green sulfur bacteria are chlorosomes. These are generally oblate spheroid organelles approximately 100-200 nm in length, 30-70 nm in width and 30-40 nm thick.[5] A single chlorosome may contain up to 250,000 bacteriochlorophyll *c/d/e* (BChl *c/d/e*) molecules[4,6,7] that are self-assembled into tube-like or lamellae

aggregates[8–14] and are enclosed within in a protein-lipid monolayer.[15] Absorption of a photon results in the creation of a molecular exciton, which is transported to the next subunit of the LHC - a baseplate, which is located on one side of the chlorosome surface. The energy is then sinked through an intermediate Fenna-Matthews-Olson (FMO) complex to a reaction center where it is used in the production of chemical compounds.

Within the semiclassical approximation of incoherent excitons (i.e. no quantum coherence), efficient light harvesting requires strong light absorption combined with the fast energy relaxation that drives the exciton towards the reaction center, protecting it from reemission and non-radiative recombination. However, recent work on green sulfur bacteria has suggested that electronic coherence may play a role in the energy transfer through the LHC. Evidence of quantum coherence between bacteriochlorophyll molecules within the FMO complex has been observed[16,17] and extensively analyzed theoretically.[18–22] Ultrafast energy transfer in the chlorosomes has also been reported.[23–25] While the latter studies do not exclude coherent exciton dynamics on femtosecond timescale it was not clearly observed in the experiments.

Strong exciton-photon coupling is the result of a coherent exchange of energy between an exciton and a resonant photonic mode. The coupling manifests as a mixing in the energetic dispersions of the cavity and exciton modes and the formation of the cavity-polariton quasiparticle which can be described as a linear mixture of the photon and exciton. The polariton energy dispersion takes the form of two 'branches' that anticross when the cavity mode energy is tuned through the exciton energy. These are the polariton branches and are termed the upper polariton branch (UPB) and lower polariton branch (LPB) for the branches that exist above and below the exciton energy respectively. The magnitude of the energetic splitting of the branches at exciton-photon resonance is the Rabi splitting energy $\hbar\Omega$. Optical microcavities provide a convenient system in which to explore the strong coupling regime due to their relatively straightforward fabrication and simple tuning of the cavity mode energy through angular dependent measurements. Typical cavity structures consist of two mirrors separated on the order of hundreds of nanometers with the excitonic material located within

the cavity. The requirements of strong coupling include a large absorption oscillator strength and narrow absorption linewidth for the exciton, and small cavity losses into leaky modes.

Strong coupling in microcavities has been demonstrated with a wide range of excitonic systems including semiconductor quantum wells,[26–28] quantum dots,[29,30] bulk semiconductors,[31,32] nanowires,[33] small organic molecules,[34–36] J-aggregates,[37–39] polymers[40,41] and molecular crystals.[42–44] Organic materials have also been shown to strongly couple to the surface plasmons of metallic films[45,46] and nanoparticles.[47,48] Recently, strong coupling between the surface plasmons of a metallic film and β-carotene molecules was demonstrated.[49] Several studies have discussed modified absorption, emission and energy transfer in natural LHCs weakly coupled with quantum dots,[50] plasmonic particles[51] and optical cavities.[52,53] In this paper we demonstrate that the exciton states in the chlorosome can be coherently coupled to the vacuum electromagnetic field confined in an optical microcavity, thereby creating polariton modes. To our knowledge this is the first demonstration of strong exciton-photon coupling in natural light-harvesting structures. In addition to the demonstration of chlorosome-cavity coupling, our work opens a new avenue to modify the energy landscape in the LHCs. We show that the energy of polariton modes can be detuned from the bare exciton states on the order of 100 meV which is comparable to the energy difference between the chlorosome and the baseplate. We suggest that such structures could be used for strong coupling of living photosynthetic bacteria with light to create 'living polaritons.'

To prepare chlorosomes for inclusion in a microcavity, they were first purified from the *Chlorobaculum tepidum* species of green sulfur bacteria, which were cultured anaerobically and phototropically using the medium as reported previously.[1] The cultures were incubated at 45°C in low intensity light (20 ± 2 μmol/m^2/s) and harvested at the steady-state of growth, from which chlorosomes were extracted from the membrane fraction using 2M NaI followed by sucrose gradient separation via ultracentrifugation at 135,000 $\times$ g for 16 h. The

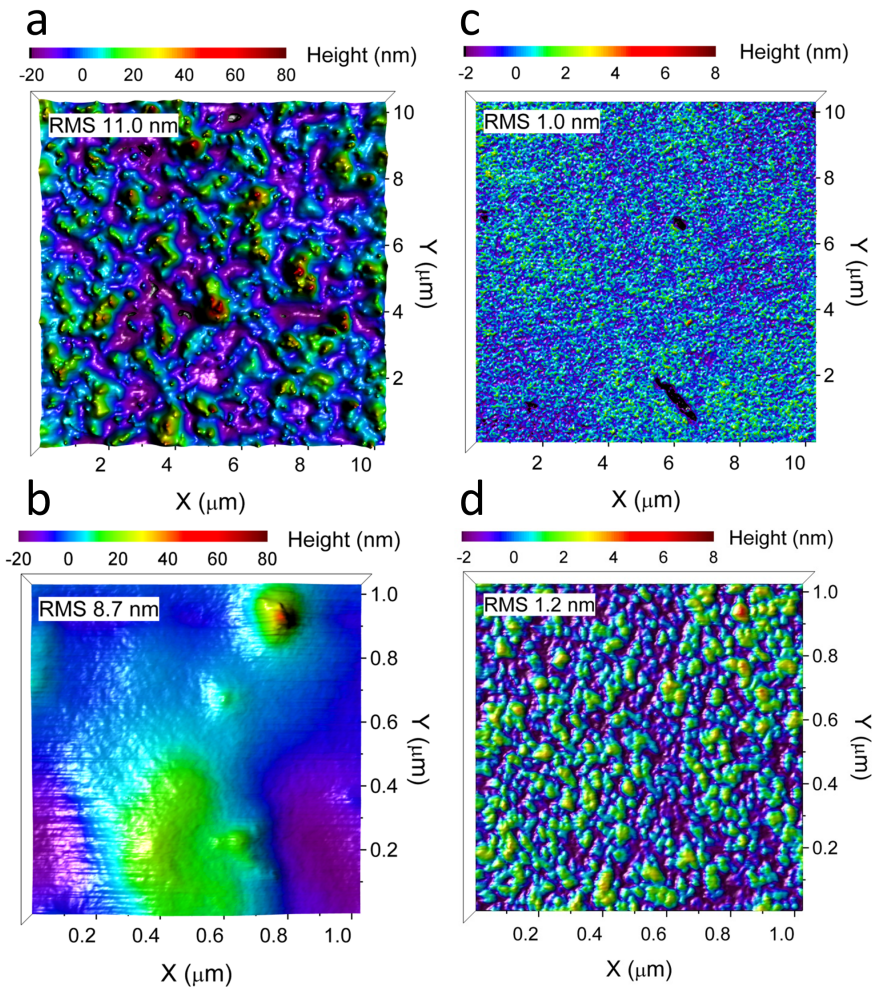

Figure 1: AFM topology images of a chlorosome containing PVA film for scan areas of (a) 10×10 μm and (b) 1×1 μm. Topology images for a pure PVA film for scan areas of (c) 10×10 μm and (d) 1×1 μm.

purified chlorosomes were characterized by room temperature UV-visible, fluorescence emission, circular dichroism (CD) spectroscopy, and dynamic light scattering (DLS) as reported previously.[14,54] The samples were then desalted and lyophilized. The chlorosomes were then dispersed in a poly(vinyl alcohol) (PVA, m_w=31K-50K, 87-89% hydrolized, Sigma Aldrich) matrix. The PVA was dissolved in deionized water at a concentration of 40 mg/ml. The lyophilized chlorosomes were mixed in the aqueous PVA solution at a concentration of 10 mg/ml with a vortex mixer before the solution was passed through a PVDF filter (0.45 μm pore size). This solution was spincast to form $\sim$200 nm thick films.

Figure 1(a) and (b) show atomic force microscope (AFM) topology maps of a chlorosome containing PVA films on length scales of 10 $\times$ 10 μm and 1 $\times$ 1 μm respectively. The film surface displays features of sizes $50 - 250$ nm, similar to the size of chlorosomes, and has a large RMS surface roughness of $\sim$10 nm with surface protrusions reaching a maximum of 100 nm. For comparison, AFM topology images of a PVA film without chlorosomes is shown in Figure 1(c) and (d) on on length scales of 10 $\times$ 10 μm and 1 $\times$ 1 μm respectively. The RMS surface roughness of this film is on the order of 1 nm with no large features visible.

To fabricate microcavities, the chlorosome-PVA solution was spincast onto a 40 nm thick thermally evaporated semitransparent silver mirror to a thickness of $\sim$205 nm. A second 40 nm thick silver mirror was evaporated directly onto the organic layer to complete the $\lambda/2$ microcavity. The cavity structure is shown in Figure 2(a), with the chlorosome, BChl *c* aggregate and BChl *c* molecule being depicted in (b), (c) and (d) respectively. A transmission electron microscope (TEM) image of the chlorosomes is shown in part (e). Part (f) shows the optical absorption of a control film of chlorosomes in PVA. An 'empty' cavity was also fabricated which contained a 200 nm thick film of PVA with no chlorosomes.

The microcavity was analysed with room temperature reflection and transmission spectroscopy. The cavity was mounted on the rotation axis of goniometer and a fiber-coupled

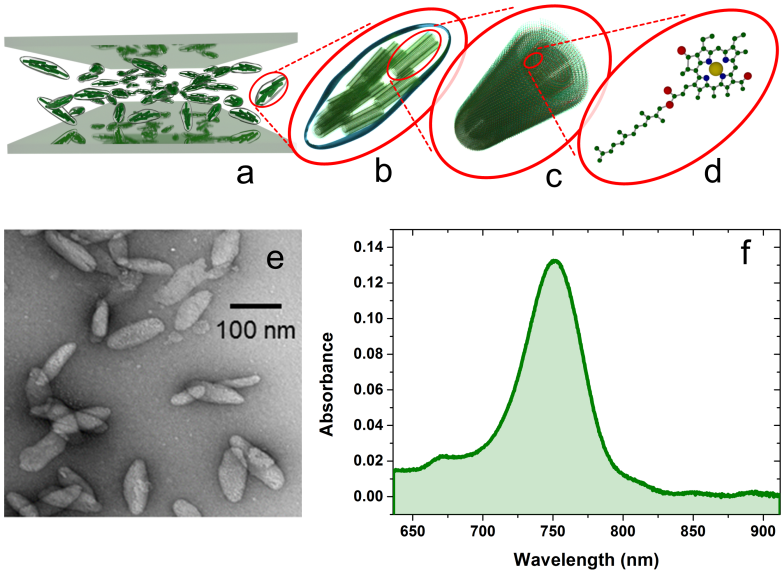

Figure 2: (a) A microcavity was fabricated which consisted of a 205 nm thick chlorosome-containing PVA film between two 40 nm thick semi-transparent silver mirrors. (b) The chlorosomes contain large aggregates of BChl *c* molecules within a protein-lipid monolayer. (c) The BChl *c* molecules (shown in (d)) self-assemble into tube-like structures. (e) TEM image of chlorosomes. (f) Absorbance of a 205 nm thick film of chlorosomes in a PVA matrix.

white light was focused to a 500 μm spot on the sample surface. For reflectivity measurements the sample was rotated whilst the reflected light was collected by optics mounted on the rotating goniometer arm. For transmission measurements, the collection arm was fixed opposite the excitation light and only the sample was rotated. The same spot on the sample was probed in reflection and transmission with an angular resolution of 2°. The collected light was analysed with a fiber-coupled CCD spectrometer (Andor Shamrock 303i). Due to the weak excitation, and the light collection optics being placed far from the sample, no photoluminescence is detected in reflectivity or transmission measurements.

Figure 3(a i) and (a ii) show the measured transmission and reflectivity measurements recorded from the empty microcavity. In both cases a single peak/dip is seen in the spectrum of each angle corresponding to the cavity mode. The linewidth of the cavity mode at 16° is ∼20 nm, corresponding to a cavity Q-factor of 40 and a photon confinement time of 15 fs. We have modelled the empty cavity transmission and reflectivity spectra with the transfer matrix method (TMM), whose output is presented in Figures 3(a iii) and (a iv) respectively (in transverse electric (TE) polarized light). The model uses a constant refractive index of 1.53 for the PVA and no absorption or scattering is included in the PVA layer. There is excellent agreement between the observed cavity dispersion and the TMM modelling. In particular, the observed mode visibility and linewidth are well reproduced by the TMM indicating that the absorption and scattering in the PVA layer is negligible, as would be expected from the high surface quality of the film revealed by AFM. The cavity mode energy (E_γ), is given by $E_\gamma(\theta) = E_\gamma(0)\left(1 - \frac{\sin^2\theta}{n_{\text{eff}}}\right)^{-\frac{1}{2}}$ where θ is the observation angle, n_{eff} is the effective intracavity refractive index and $E_\gamma(0)$ is the cavity cutoff energy which for a $\lambda/2$ cavity of length L is given by $E_\gamma(0) = \frac{hc}{2n_{\text{eff}}L}$. The fit to the cavity mode energy is shown as a red dashed line in Figure 3(a).

The angular dependent transmission and reflectivity spectra of the microcavity containing chlorosomes are shown in Figures 3 (b i) and (b ii) respectively. Two peaks/dips can be

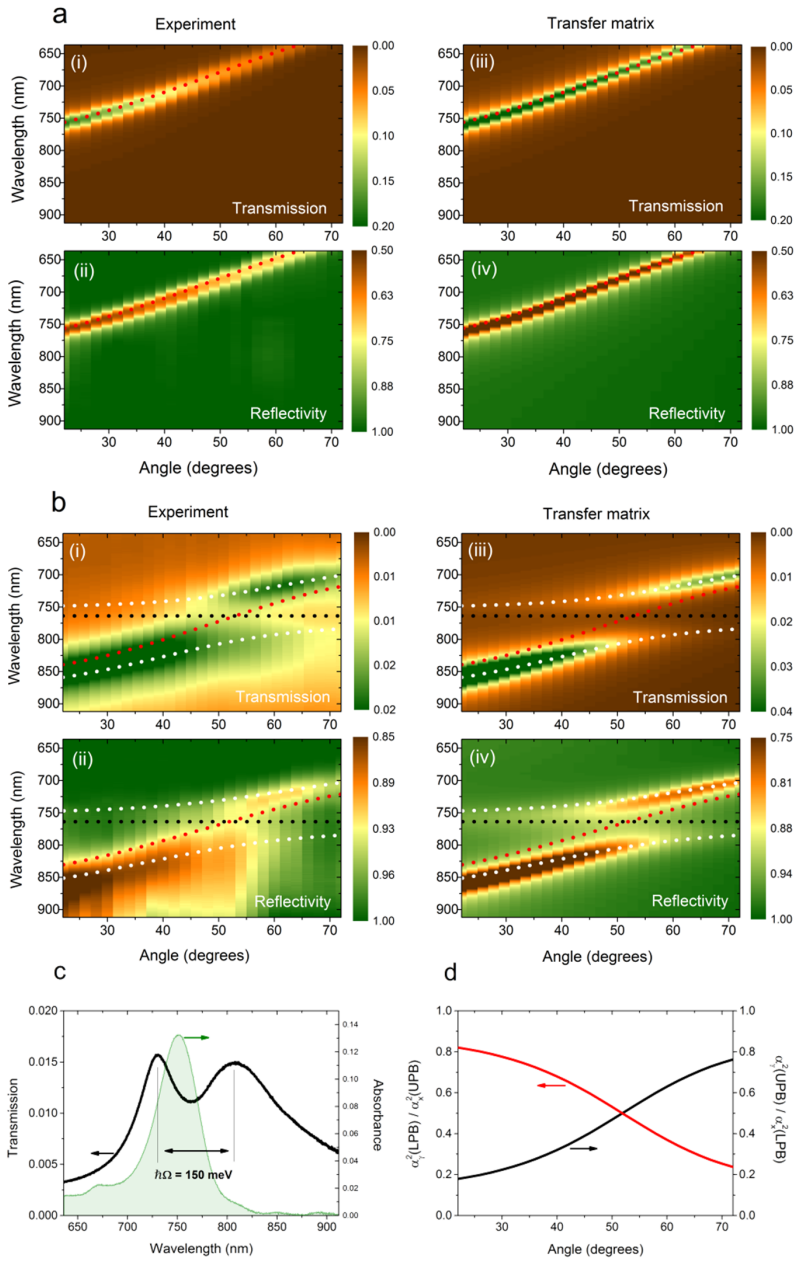

Figure 3: (a) Experimental angular dependent (i) transmission and (ii) reflectivity of an 'empty' PVA cavity and TMM modelled spectra of the same cavity in (iii) transmission and (iv) reflectivity. Fitted cavity dispersion is shown as a red dashed line. (b) Experimental angular dependent (i) transmission and (ii) reflectivity of a chlorosome-containing PVA cavity and TMM modelled spectra of the same cavity in (iii) transmission and (iv) reflectivity. Fitted cavity mode and exciton energies are shown as dashed red and black lines respectively, and polariton branch dispersions are shown as white dashed lines. (c) Strongly-coupled transmission spectrum at resonance (54°). The chlorosome film absorbance is also shown in green. (d) Mixing coefficients of the polariton branches.

seen clearly in the data that undergo an anticrossing about the chlorosome exciton energy, indicating that the system is operating in the strong-coupling regime. The energy of the polariton branches can be described by the coupled oscillator model.[55]

$$\begin{pmatrix} E_\gamma(\theta) & \hbar\Omega/2 \\ \hbar\Omega/2 & E_\mathrm{x} \end{pmatrix} \begin{pmatrix} \alpha_\gamma(\theta) \\ \alpha_\mathrm{x}(\theta) \end{pmatrix} = E_\mathrm{p}(\theta) \begin{pmatrix} \alpha_\gamma(\theta) \\ \alpha_\mathrm{x}(\theta) \end{pmatrix}, \tag{1}$$

where E_x is the exciton energy, $\hbar\Omega$ is the Rabi splitting energy, E_p is the polariton energy and α_x^2 and α_γ^2 are the mixing coefficients which describe the fraction of exciton and photon in the polariton state and can be shown to be given by $\alpha_\gamma^2 = \frac{E_\gamma - E_\mathrm{p}}{E_\gamma + E_\mathrm{x} - 2E_\mathrm{p}}$, $\alpha_\mathrm{x}^2 = 1 - \alpha_\gamma^2$. The observed transmission peak positions are fitted with Eqn. 1, with $E_\gamma(0)$, n_eff, E_x and $\hbar\Omega$ as fitting parameters. We find that the coupled system displays a Rabi splitting energy of $\hbar\Omega$ =156 meV and detuning of $\Delta = E_\gamma(0) - E_\mathrm{x} = -164$ meV. The fitted polariton branch positions are shown as white dashed lines in Figure 3(b), with the photon mode and exciton wavelengths shown with red and black dashed lines respectively. The chlorosome exciton energy E_x found from the fit is redshifted by approximately 12 nm with respect to absorption peak. It has previously been observed that in strongly-coupled microcavities containing J-aggregates the exciton resonance appears blueshifted with respect to the absorption peak.[56,57] This was ascribed to the asymmetric shape of the absorption band and residual oscillator strength lying in higher energy states. A similar effect may be responsible for the redshift observed here, with some oscillator strength being at lower energy than the absorption peak. The cavity transmission spectrum at the resonance angle (54°) is shown in Figure 3(c). We note that the effective refractive index of the chlorosome containing film is found through fitting to the the two-level model to be approximately 1.8 which leads to an extended optical path length in the cavity in comparison to the PVA-only cavity, resulting in the cavity mode energy being redshifted. The excitonic and photonic mixing coefficients of the polariton branches are shown in Figure 3(d).

TMM was again used to model to chlorosome cavity system. The film absorption was

fitted to a Lorentzian oscillator model which allows the real (n) and imaginary (k) parts of the refractive index to calculated. The modelled transmission and reflectivity spectra are shown in Figures 3(b iii) and (b iv) respectively. While the dispersions of the polariton branches show good agreement with the experimentally observed spectra, the linewidths of the experimental polariton branches are considerably broadened in comparison with the TMM model (72 nm in comparison to 23 nm at 16° in transmission). This is due to the large degree of surface roughness in the chlorosome-containing film resulting in in-plane scattering which reduces the Q-factor of the cavity and hence broadens the cavity mode and polariton linewidths.

We can account for the scattering in the TMM model in a phenomenological way by incorporating a background extinction into the imaginary part of the film refractive index. We do this for the chlorosome cavity and find that a background extinction of 0.06 reproduces observed linewidths. Importantly, the Rabi splitting (75 nm) remains larger than the broadened cavity mode linewidth despite the additional scattering.[58] From TMM we find that the scattering reduces the cavity Q-factor to 12 (photon confinement time of 5 fs). Strong coupling has previously been observed in metallic cavities with a similar Q-factor using J-aggregates as the coupling medium.[59] It should be noted that the coupling strength is in fact maximized when the linewidths of the photon and exciton are well matched,[58,60] hence the broadened cavity mode linewidth is not too detrimental to the strong coupling.

The magnitude of the Rabi splitting energy may be used to gain an order-of-magnitude estimate of the number of chlorosomes involved in the formation of the polariton mode. The Rabi splitting energy is given by Eqn. 2,[61] where N is the number of coupled oscillators, $\vec{\mu}$ is the dipole moment of the coupled oscillators, V is the mode volume of the cavity mode and $\hat{E}$ is a unit vector parallel to the polarization of the electric field in the cavity.

$$\hbar\Omega = 2\left(\vec{\mu}\cdot\hat{E}\right)\sqrt{N}\left(\frac{\pi\hbar c}{n_{\text{eff}}^2\lambda\epsilon_0 V}\right)^{\frac{1}{2}} \tag{2}$$

We estimate the $\lambda/2$ mode volume[62] to be 15.7 $(\lambda/n_{\text{eff}})^3$ (assuming mirror reflectivities

of 95% as found through TMM) where $n_{\text{eff}} = 1.8$. This is an upper limit as it does not take into account in-plane scattering which will reduce the mode volume. We assume that each chlorosome contains an average of 200,000 BChl c monomers, the square of the monomer transition dipole $|\vec{\mu}|^2 = 30$ D^2,[63] and the average angle between the transition dipoles and the chlorosome's main axis is about 28°.[64] It is likely that the spin coating process does result in some preferential orientation of chlorosomes in the plane of the film. Then, the number of coherently coupled chlorosomes estimated with Eqn. 2 and assuming that the chlorosomes are aligned parallel to the confined E-field is ∼1000. It should be noted that the intermolecular coupling in the aggregate of BChls only redistributes the oscillator strength between the electronic transitions keeping the product $|\vec{\mu}|^2 N$ the same. Thus, the transition dipoles $\vec{\mu}$ and the number of states N in Eqn. 2 can be taken to be those of the BChl monomers, provided that the cavity frequency is shifted from the monomer transition to the absorption spectrum of the aggregate, and the cavity line is broad enough such that the optical mode interacts resonantly with all optically allowed electronic transitions.

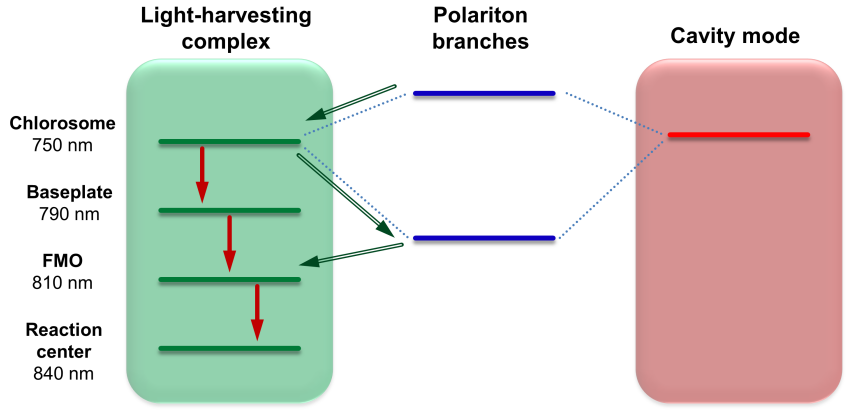

Figure 4: Energy level diagram of a green sulfur bacteria LHC coupled to an optical cavity. The red dashed arrows show the energy transport pathway in an unperturbed LHC. Strong interaction of the cavity photons with the chlorosome exciton states result in formation of polariton branches with the Rabi splitting about 150 meV. The green arrows show possible energy pathways in the coupled system.

Finally, we discuss the possibility to modify the energy transfer pathways in LHCs of green sulfur bacteria using optical microcavities. A schematic of the energy levels within the light-harvesting system is shown in Figure 4 (green box). When the chlorosome strongly couples to the cavity mode, two new energy levels are created about the chlorosome energy. Polariton states on the lower branch are shifted to lower energy than the uncoupled exciton and hence can overlap with the absorption band of the chlorosome baseplate at ∼790 nm and the Fenna-Matthews-Olson complex at ∼810 nm. This may change the conventional paradigm of light-harvesting when the photons are absorbed by the chlorosome and then consequently transported through several subunits of the LHC to the case when the energy flows from the polariton states to the baseplate or to the FMO complexes. The energetic separation between the chlorosome polariton states and the baseplate/FMO can be easily tuned through angle, potentially allowing the efficiency of this process to be enhanced or suppressed within the same microcavity structure and without modification of the molecular structure. As such this represents a new channel to explore the interaction of biological systems and light. Relatively little is known about the energy transfer efficiency of excitons throughout the entire LHC, and it will be interesting to see if bypassing certain exciton states in the LHC will increase the efficiency of the antenna. This may in turn have implications for the rate of bacterial growth. Since there are approximately 200-250 chlorosomes in each *Chlorobaculum tepidum* bacteria,[65] it is expected that if ∼4 bacteria could occupy the cavity mode volume, they could strongly couple to the cavity. The bacterial cell is 0.6-0.8 μm long,[66] hence it may indeed be possible to reach this limit to create 'living polaritons' and therefore directly investigate the effect of tuning the LHC energy levels on bacterial growth.

In conclusion we have demonstrated strong coupling between a low-Q optical cavity and the chlorosome of green sulfur bacteria with a Rabi splitting of approximately 150 meV. The chlorosomes cause large amounts of scattering into the microcavity system, however this damping is not strong enough to destroy the strong coupling. It is worth noting that is it the excited state of the chlorosome that couples to the photon and not simply the excited

state of the BChl *c* molecule which has an absorption peak at 667 nm.[67,68] We believe this to be the first demonstration of strong exciton-photon coupling in a large biological system. The mixed polariton state of light-harvesting antenna and photon may present a new system for studying the light-matter interaction that is ultimately responsible for the process of photosynthesis. We have recently shown that polaritons states can form an efficient energy relaxation pathway between spatially and energetically separated exciton species,[69] hence this demonstration of strong-coupling in a biological system may allow for artificial light harvesting devices that utilize biological components. Finally, since the density of chlorosomes within the green sulfur bacteria is high, it may be possible to strongly-couple a living bacteria to a cavity mode resulting in a 'living polariton'.

Supporting Information Available: Light harvesting complex and tubular bacteriochlorophyll aggregate structure, and measured/calculated chlorosome absorption and circular dichromism spectra. This material is available free of charge via the Internet at http://pubs.acs.org.

D.M.C, R.A.T and J.M.S gratefully acknowledge the Oxford Martin School for financial support. J.K.T. is supported by start-up funds from Clark University. S.K.S. and A.A.G. acknowledge Defense Threat Reduction Agency Grant HDTRA1-10-1-0046. S.K.S. also grateful to the Russian Government Program of Competitive Growth of Kazan Federal University. A.A.G. thanks the Center for Excitonics, an Energy Frontier Research Center funded by the U.S. Department of Energy, Office of Science and Office of Basic Energy Sciences, under Award Number DE-SC0001088. R.T.G thanks EPSRC for a DTG Studentship, D.G.L thanks EPSRC for continued support.

References

(1) Overmann, J. *The Prokaryotes*, 3rd ed.; Springer, New York, 2006; Vol. 7; pp 359 – 378.

(2) Overmann, J.; Cypionka, H.; Pfennig, N. *Limnology and oceanography* **1992**, *37*, 150–155.

(3) Beatty, J. T.; Overmann, J.; Lince, M. T.; Manske, A. K.; Lang, A. S.; Blankenship, R. E.; Van Dover, C. L.; Martinson, T. a.; Plumley, F. G. *Proceedings of the National Academy of Sciences of the United States of America* **2005**, *102*, 9306–10.

(4) Huh, J.; Saikin, S. K.; Brookes, J. C.; Valleau, S.; Fujita, T.; Aspuru-Guzik, A. *Journal of the American Chemical Society* **2014**, *136*, 2048–2057.

(5) Kouyianou, K.; De Bock, P.-J.; Mller, S. A.; Nikolaki, A.; Rizos, A.; Krzyžánek, V.; Aktoudianaki, A.; Vandekerckhove, J.; Engel, A.; Gevaert, K.; Tsiotis, G. *PROTEOMICS* **2011**, *11*, 2867–2880.

(6) Oostergetel, G.; Amerongen, H.; Boekema, E. *Photosynthesis Research* **2010**, *104*, 245–255.

(7) Frigaard, N.-U.; Chew, A.; Li, H.; Maresca, J.; Bryant, D. *Photosynthesis Research* **2003**, *78*, 93–117.

(8) Holzwarth, A. R.; Schaffner, K. *Photosynthesis Research* **1994**, *41*, 225–233.

(9) Frese, R.; Oberheide, U.; van Stokkum, I.; van Grondelle, R.; Foidl, M.; Oelze, J.; van Amerongen, H. *Photosynthesis Research* **1997**, *54*, 115–126.

(10) Pšenčìk, J.; Ikonen, T.; Laurinmäki, P.; Merckel, M.; Butcher, S.; Serimaa, R.; Tuma, R. *Biophysical Journal* **2004**, *87*, 1165–1172.

(11) Linnanto, J. M.; Korppi-Tommola, J. E. *Photosynthesis Research* **2008**, *96*, 227–245.

(12) Ganapathy, S.; Oostergetel, G. T.; Wawrzyniak, P. K.; Reus, M.; Gomez Maqueo Chew, A.; Buda, F.; Boekema, E. J.; Bryant, D. A.; Holzwarth, A. R.; de Groot, H. J. M. *Proceedings of the National Academy of Sciences* **2009**, *106*, 8525–8530.

(13) Ganapathy, S.; Oostergetel, G. T.; Reus, M.; Tsukatani, Y.; Gomez Maqueo Chew, A.; Buda, F.; Bryant, D. A.; Holzwarth, A. R.; de Groot, H. J. M. *Biochemistry* **2012**, *51*, 4488–4498.

(14) Tang, J. K.; Saikin, S. K.; Pingali, S. V.; Enriquez, M. M.; Huh, J.; Frank, H. A.; Urban, V. S.; Aspuru-Guzik, A. *Biophysical Journal* **2013**, *105*, 1346–1356.

(15) Huber, V.; Katterle, M.; Lysetska, M.; Wrthner, F. *Angewandte Chemie International Edition* **2005**, *44*, 3147–3151.

(16) Engel, G. S.; Calhoun, T. R.; Read, E. L.; Ahn, T.-K.; Mancal, T.; Cheng, Y.-C.; Blankenship, R. E.; Fleming, G. R. *Nature* **2007**, *446*, 782–786.

(17) Brixner, T.; Stenger, J.; Vaswani, H. M.; Cho, M.; Blankenship, R. E.; Fleming, G. R. *Nature* **2005**, *434*, 625–8.

(18) Mohseni, M.; Rebentrost, P.; Lloyd, S.; Aspuru-Guzik, A. *The Journal of chemical physics* **2008**, *129*, 174106.

(19) Plenio, M. B.; Huelga, S. F. *New J. Phys.* **2008**, *10*, 113019.

(20) Ishizaki, A.; Fleming, G. R. *J. Chem. Phys.* **2009**, *130*, 234111.

(21) Olbrich, C.; Strümpfer, J.; Schulten, K.; Kleinekathöfer, U. *The journal of physical chemistry letters* **2011**, *2011*, 1771–1776.

(22) Ritschel, G.; Roden, J.; Strunz, W. T.; Aspuru-Guzik, A.; Eisfeld, A. *The Journal of Physical Chemistry Letters* **2011**, *2*, 2912–2917.

(23) Savikhin, S.; van Noort, P. I.; Zhu, Y.; Lin, S.; Blankenship, R. E.; Struve, W. S. *Chemical Physics* **1995**, *194*, 245–258.

(24) Psencík, J.; Ma, Y.-Z.; Arellano, J. B.; Hála, J.; Gillbro, T. *Biophysical journal* **2003**, *84*, 1161–79.

(25) Dostal, J.; Mancal, T.; Augulis, R.; Vacha, F.; Psencik, J.; Zigmantas, D. *Journal of the American Chemical Society* **2012**, *134*, 11611–11617.

(26) Weisbuch, C.; Nishioka, M.; Ishikawa, A.; Arakawa, Y. *Phys. Rev. Lett.* **1992**, *69*, 3314–3317.

(27) Houdré, R.; Weisbuch, C.; Stanley, R. P.; Oesterle, U.; Pellandini, P.; Ilegems, M. *Phys. Rev. Lett.* **1994**, *73*, 2043–2046.

(28) Tassone, F.; Piermarocchi, C.; Savona, V.; Quattropani, A.; Schwendimann, P. *Phys. Rev. B* **1997**, *56*, 7554–7563.

(29) Reithmaier, J. P.; Sek, G.; Loffler, A.; Hofmann, C.; Kuhn, S.; Reitzenstein, S.; Keldysh, L. V.; Kulakovskii, V. D.; Reinecke, T. L.; Forchel, A. *Nature* **2004**, *432*, 197–200.

(30) Peter, E.; Senellart, P.; Martrou, D.; Lemaître, A.; Hours, J.; Gérard, J. M.; Bloch, J. *Phys. Rev. Lett.* **2005**, *95*, 067401.

(31) Butté, R.; Christmann, G.; Feltin, E.; Carlin, J.-F.; Mosca, M.; Ilegems, M.; Grandjean, N. *Phys. Rev. B* **2006**, *73*, 033315.

(32) Christopoulos, S.; von Högersthal, G. B. H.; Grundy, A. J. D.; Lagoudakis, P. G.; Kavokin, A. V.; Baumberg, J. J.; Christmann, G.; Butté, R.; Feltin, E.; Carlin, J.-F.; Grandjean, N. *Phys. Rev. Lett.* **2007**, *98*, 126405.

(33) Das, A.; Heo, J.; Bayraktaroglu, A.; Guo, W.; Ng, T.-K.; Phillips, J.; Ooi, B. S.; Bhattacharya, P. *Opt. Express* **2012**, *20*, 11830–11837.

(34) Lidzey, D. G.; Bradley, D. D. C.; Skolnick, M. S.; Virgili, T.; Walker, S.; Whittaker, D. M. *Nature* **1998**, *395*, 53–55.

(35) Savvidis, P. G.; Connolly, L. G.; Skolnick, M. S.; Lidzey, D. G.; Baumberg, J. J. *Phys. Rev. B* **2006**, *74*, 113312.

(36) Daskalakis, K. S.; Maier, S. A.; Murray, R.; Kéna-Cohen, S. *Nature Materials* **2014**, *13*, 271278.

(37) Lidzey, D. G.; Bradley, D. D. C.; Virgili, T.; Armitage, A.; Skolnick, M. S.; Walker, S. *Phys. Rev. Lett.* **1999**, *82*, 3316–3319.

(38) Schouwink, P.; Berlepsch, H. V.; Dähne, L.; Mahrt, R. F. *Chemical Physics Letters* **2001**, *344*, 352 – 356.

(39) Tischler, J. R.; Bradley, M. S.; Bulović, V.; Song, J. H.; Nurmikko, A. *Phys. Rev. Lett.* **2005**, *95*, 036401.

(40) Takada, N.; Kamata, T.; Bradley, D. D. C. *Applied Physics Letters* **2003**, *82*, 1812–1814.

(41) Plumhof, J. D.; St oferle, T.; Mai, L.; Scherf, U.; Mahrt, R. F. *Nature Materials* **2014**, *13*, 247252.

(42) Holmes, R. J.; Forrest, S. R. *Phys. Rev. Lett.* **2004**, *93*, 186404.

(43) Kéna-Cohen, S.; Davanço, M.; Forrest, S. R. *Phys. Rev. Lett.* **2008**, *101*, 116401.

(44) Kéna-Cohen, S.; Forrest, S. *Nature Photonics* **2010**, *4*, 371–375.

(45) Bellessa, J.; Bonnand, C.; Plenet, J. C.; Mugnier, J. *Phys. Rev. Lett.* **2004**, *93*, 036404.

(46) Bonnand, C.; Bellessa, J.; Plenet, J. C. *Phys. Rev. B* **2006**, *73*, 245330.

(47) Fofang, N. T.; Park, T.-H.; Neumann, O.; Mirin, N. A.; Nordlander, P.; Halas, N. J. *Nano Letters* **2008**, *8*, 3481–3487.

(48) Djoumessi Lekeufack, D.; Brioude, A.; Coleman, A. W.; Miele, P.; Bellessa, J.; De Zeng, L.; Stadelmann, P. *Applied Physics Letters* **2010**, *96*, 253107.

(49) Baieva, S.; Ihalainen, J. A.; Toppari, J. J. *The Journal of Chemical Physics* **2013**, *138*, 044707.

(50) Nabiev, I.; Rakovich, A.; Sukhanova, A.; Lukashev, E.; Zagidullin, V.; Pachenko, V.; Rakovich, Y. P.; Donegan, J. F.; Rubin, A. B.; Govorov, A. O. *Angewandte Chemie International Edition* **2010**, *49*, 7217–7221.

(51) Carmeli, I.; Lieberman, I.; Kraversky, L.; Fan, Z.; Govorov, A. O.; Markovich, G.; Richter, S. *Nano Letters* **2010**, *10*, 2069–2074.

(52) Caruso, F.; Saikin, S. K.; Solano, E.; Huelga, S. F.; Aspuru-Guzik, A.; Plenio, M. B. *Phys. Rev. B* **2012**, *85*, 125424.

(53) Konrad, A.; Trost, A.-L.; Skandary, S.; Hussels, M.; Meixner, A. J.; Karapetyan, N. V.; Brecht, M. *Phys. Chem. Chem. Phys.* **2014**, *16*, 6175–6181.

(54) Tang, J. K. H.; Xu, Y.; Muhlmann, G.; Zare, F.; Khin, Y.; Tam, S. *Photosynthesis Research* **2013**, *115*, 23–41.

(55) Skolnick, M. S.; Fisher, T. A.; Whittaker, D. M. *Semicond. Sci. Technol.* **1998**, *13*, 645.

(56) Armitage, A.; Lidzey, D.; Bradley, D.; Virgili, T.; Skolnick, M.; Walker, S. *Synthetic Metals* **2000**, *111112*, 377 – 379.

(57) Coles, D. M.; Michetti, P.; Clark, C.; Tsoi, W. C.; Adawi, A. M.; Kim, J.-S.; Lidzey, D. G. *Advanced Functional Materials* **2011**, *21*, 3691–3696.

(58) Houdré, R.; Stanley, R. P.; Oesterle, U.; Ilegems, M.; Weisbuch, C. *Phys. Rev. B* **1994**, *49*, 16761–16764.

(59) Hobson, P. A.; Barnes, W. L.; Lidzey, D. G.; Gehring, G. A.; Whittaker, D. M.; Skolnick, M. S.; Walker, S. *Applied Physics Letters* **2002**, *81*, 3519–3521.

(60) Kelkar, P. V.; Kozlov, V. G.; Nurmikko, A. V.; Chu, C.-C.; Han, J.; Gunshor, R. L. *Phys. Rev. B* **1997**, *56*, 7564–7573.

(61) Fox, M. *Quantum Optics - An Introduction*; Oxford Master Series, 2006.

(62) Ujihara, K. *Japanese Journal of Applied Physics* **1991**, *30*, L901–L903.

(63) Prokhorenko, V.; Steensgaard, D.; Holzwarth, A. *Biophysical Journal* **2000**, *79*, 2105 – 2120.

(64) Furumaki, S.; Vacha, F.; Habuchi, S.; Tsukatani, Y.; Bryant, D. a.; Vacha, M. *Journal of the American Chemical Society* **2011**, *133*, 6703–10.

(65) Schaechter, M. *Encyclopedia of Microbiology*, 3rd ed.; Academic Press/Elsevier, 2009; Vol. 2; pp 404–425.

(66) Imhoff, J. F. *International Journal of Systematic and Evolutionary Microbiology* **2003**, *53*, 941–951.

(67) Miller, M.; Gillbro, T.; Olson, J. M. *Photochemistry and Photobiology* **1993**, *57*, 98–102.

(68) Balaban, T. S.; Holzwarth, A. R.; Schaffner, K. *Journal of Molecular Structure* **1995**, *349*, 183 – 186, Molecular Spectroscopy and Molecular Structure 1994.

(69) Coles, D. M.; Somaschi, N.; Michetti, P.; Clark, C.; Lagoudakis, P. G.; Savvidis, P. G.; Lidzey, D. G. *Nature Materials* **2014**,